VEHICLE COMPATIBILITY ASSESSMENT USING TEST DATA OF FULL FRONTAL VEHICLE-TO-VEHICLE AND VEHICLE-TO-FULL WIDTH DEFORMABLE BARRIER IMPACTS

Saeed Barbat
Xiaowei Li
Steve Reagan
Priya Prasad
Passive Safety Research and Advanced Engineering
Ford Motor Company
United States
Paper Number 07-0348

ABSTRACT

This paper provides an update of Ford's research activity in vehicle compatibility. Vehicle manufacturers extrapolate compatibility performance in real-world accidents using data from controlled crash test environments. Several test procedures and various compatibility measures which use data obtained from rigid or deformable barrier tests to quantify expected compatibility with smaller vehicles have been previously proposed. The purpose of this research is to examine potential compatibility measures obtained from vehicle-to-barrier impact as well as to evaluate the effectiveness of the "BlockerBeam®" in vehicle-to-vehicle impact. The BlockerBeam® is one method of designing a Secondary Energy Absorbing Structure (SEAS). The BlockerBeam® is attached to the front end of the rail/frame of an SUV or full size pick-up below the bumper. It can enhance structural interaction and reduce override during frontal impact with a passenger car.

The current research presents data analyses obtained from vehicle-to-barrier and vehicle-to-vehicle crash tests to develop assessment methodologies intended to evaluate vehicle compatibility. Full size heavy-duty pick-ups with and without a BlockerBeam® were instrumented and tested in 57 km/h frontal impacts against a full width deformable barrier. The barrier consisted of 128 high resolution, 125 mm by 125 mm load cells arranged in a 16 row by 8 column array. Identical full size pick-ups with and without a BlockerBeam® were also tested in vehicle-to-vehicle full frontal impact. In these tests, the impact speed of the bullet vehicle (full size heavy-duty pick-up) was set to a value intended to induce a 56 kph velocity change in the stationary target vehicle (small size 4-door sedan). The bullet and target vehicles were equipped with instrumented 50^{th}% dummies in the mid-position for the drivers and 5^{th}% dummies in the full forward position for the passengers.

Test data collected from load cells in the barrier tests was reviewed and analyzed to evaluate potential compatibility measures for use in assessing vehicle-to-vehicle crashes. Correlation between barrier test results and vehicle-to-vehicle test results for assessment of compatibility measures and test procedures is discussed.

1. INTRODUCTION

On February 11-12, 2003, the Alliance of Automobile Manufacturers (AAM) and the Insurance Institute for Highway Safety (IIHS) cosponsored an international meeting in Washington D.C. on enhancing vehicle-to-vehicle crash compatibility. It was decided during the meeting to pursue a concerted industry-wide effort to develop performance criteria to further enhance vehicle compatibility. The participants agreed to set up two technical working groups of experts to develop initiatives and actions. One working group was established to address ways to improve compatibility in front-to-side crashes, the other to address front-to-front crashes [1].

The first year's research of the TWG resulted in development and implementation of the Phase I requirements that were announced on December 3, 2003 [2] as a first step towards improving geometrical compatibility. These requirements state that participating manufacturers will begin designing light trucks in accordance with one of the following two geometric alignment alternatives, with the light truck at unloaded vehicle weight (as defined in 49 CFR 571.3):

OPTION 1: The light truck's primary frontal energy-absorbing structure shall overlap at least 50 percent of the Part 581 zone AND at least 50 percent of the light truck's primary frontal energy-absorbing structure shall overlap the Part 581 zone (if the primary frontal energy-absorbing structure of the light truck is greater than 8 inches tall, engagement with the entire Part 581 zone is required), OR,
OPTION 2: If a light truck does not meet the criteria of Option 1, there must be a secondary energy-absorbing structure (SEAS), connected to the primary structure, whose lower edge shall be no higher than the bottom of the Part 581 bumper zone.

Phase II research of the TWG focused on the development of specification and criteria for SEAS. This secondary structure shall withstand a load of at least 100 KN exerted by a loading device, as described in reference [1], Appendix A, before this loading device travels 400 mm as measured from a vertical plane at the forward-most point of the significant structure of the vehicle.

Beginning September 1, 2009, 100 percent of each participating manufacturer's new light truck up to 10,000 pounds Gross Vehicle Weight Rating (GVWR), with limited exceptions, intended for sale in the United States and Canada will be designed in accordance with either geometric alignment Option 1 or Option 2.

Ford Motor Company had already introduced a "BlockerBeam®" concept in their 2000 year model full sized SUV (as a means to improve vehicle compatibility through structural interaction during frontal impacts with passenger cars). The BlockerBeam® is a Secondary Energy Absorbing Structure (SEAS) attached to the front end of the rail/frame of an SUV or full size pick-up below the bumper. It has the potential to reduce override. Ford had migrated and implemented the BlockerBeam® concept in their 2001 production heavy-duty pick-ups. This particular design among others bring Ford's full size SUV and heavy-duty pick-ups into compliance with the Alliance Phase I option II requirements.

Phase III research for the TWG has been focused on the development of test assessment methodologies and metrics to evaluate vehicle compatibility. Previous research focusing on the development of test procedures for evaluating vehicle compatibility was reported by Barbat, et. al. [3, 4] and Edwards, et. al. [5]. Test and simulation results obtained from frontal impacts with various Load Cell Walls (LCW) and from vehicle-to-vehicle impacts to support phase III research were previously analyzed by TWG members and presented during the 19th ESV conference held in Washington D.C. in 2005 [1]. The Average Height of Force (AHOF) introduced by Digges et. al. [6] and NHTSA [7, 8] as a compatibility metric was the focus of the TWG investigation. Initial finding was that AHOF alone was an insufficient metric and did not correlate with the Aggressivity Metric (AM) defined by NHTSA [1]. Other metrics obtained from LCW such as force homogeneity within a defined corridor and enforcing force limits in certain load cell rows were studied. Currently alternative metrics and test procedures are under investigation by the TWG [9].

The purpose of the current Ford's research falls into two folds: First is to evaluate the real-world effectiveness of the BlockerBeam® in vehicle-to-vehicle frontal and side crashes. Secondly, to evaluate various metrics from vehicle-to-barrier tests, Edwards [10], and vehicle-to-vehicle crash tests that could explain the accident data.

Full size, heavy-duty pick-ups with and without a BlockerBeam® were instrumented and tested in a 57 kph frontal impact against a full width deformable barrier at PMG by Transport Canada (TC). The barrier consisted of 128 high resolution, 125 mm by 125 mm load cells arranged in a 16 row by 8 column array. Identical full size heavy-duty pick-ups with and without a BlockerBeam® were selected to be the bullet vehicles in vehicle-to-vehicle full frontal impacts conducted at Ford.

The struck target vehicle was selected to be a small size 4-door sedan. The bullet and target vehicles were equipped with instrumented 50th% dummies in the mid-position for the drivers and 5th% dummies in full forward position for the passengers. Details of test procedures, data analyses obtained from Load Cell Wall barrier and full frontal collinear vehicle-to-vehicle impact to assess compatibility metrics will be discussed in the following sections.

2. REAL-WORLD EFFECTIVNESS OF FORD'S BlockerBeam® IN IMPROVING VEHICLE COMPATIBILITY

The effect of adding secondary energy absorbing structures, SEAS (one of the recommendations of TWG) to Light Truck Vehicle (LTVs) was evaluated by comparing the collision performance of LTVs with and without Ford's BlockerBeam® SEAS in 1999-2003 FARS data for collisions involving:

- One light passenger vehicle with at least one non-ejected fatal occupant and "motor vehicle" coded as 'most harmful event', and

- One collision partner from models and the model years of interest: Ford F250 and Ford F350 pick-ups from model years 1999-2000 (without BlockerBeam®) and 2001-03 (with BlockerBeam®).

The cases selected as 'frontal impact' are identified by principal impact direction (or initial impact direction, if principal impact direction was unknown) coded as 11, 12, or 1 o'clock. The registered vehicle years (RVY) for collision partner are calculated from R. L. Polk National Vehicle Population Profile.

Table 1: Effect of BlockerBeam®; Front-to-Front Crashes

Collision Partner	Crashes		Rate per 10k RVY		P-value
	MY99-00	MY01-03	MY99-00	MY01-03	Ha: p1>p2
F-250	95	38	0.55	0.43	0.11
F-350	35	12	0.64	0.38	0.06
Control Group	36	48	0.53	0.54	0.52

In Table 1, a significant reduction in fatality rates is observed for vehicles with the added BlockerBeam®, although this data by itself is not sufficient to identify a single factor as the cause for this reduction. The data for a control group consisting of a pick-up truck similar to the F-series trucks above is also shown. This truck does not conform to the EVC recommendations and did not have any significant change in its structural height in the years under study. The data shows that for the control group, no statistically significant changes in its crash rates occurred.

Similar data is shown in Table 2 for the cases where the fronts of LTVs impacted the near side of other vehicles. Again, the effect of adding a BlockerBeam® to the LTV is seen to provide a significant reduction in the fatality rate in the struck vehicle.

Table 2: Effect of BlockerBeam®; Front-to-Near Side Impacts with Near-Side Fatalities

Collision Partner	Crashes		Rate per 10k RVY		P-value
	MY99-00	MY01-03	MY99-00	MY01-03	Ha: p1>p2
F-250	98	34	0.56	0.39	0.03

3. VEHICLE-TO-BARRIER CRASH TESTS SETUP AND PROCEDURES

Table 3 provides the significant test information regarding the mass, impact velocity, and ride heights of the two heavy-duty pick-ups considered in this test sequence. The test setup is illustrated in Figures 1A through 1C. A deformable face honeycomb material is attached to a rigid, load cell equipped barrier. The specifications of the deformable face, which consists of two 150 mm thick layers of aluminum honeycomb, are the same as those developed by Transport Research Laboratory in the U.K. (TRL). The stiffness of the layers is 0.34 MPa and 1.71 MPa for the front and rear layers, respectively. The second layer of the baseline barrier is segmented along each load cell row and column, meaning this deformable layer will not transfer load to adjacent cells.

Table 3: Test Conditions for Full-Frontal Vehicle-to-Barrier Impact Test.

		Heavy Duty Pickup with SEAS	Heavy Duty Pickup without SEAS
Vehicle Configuration	Mass (kg)	3185.6	3184.6
	Impact velocity (kph)	57.47	57.39
	Ride Height (mm) (Left / Right)	Front 995 / 995 Rear 1018 / 1020	Front 994 / 999 Rear 1017 / 1025
Height of the first row of Load Cell Wall		330 mm	330 mm

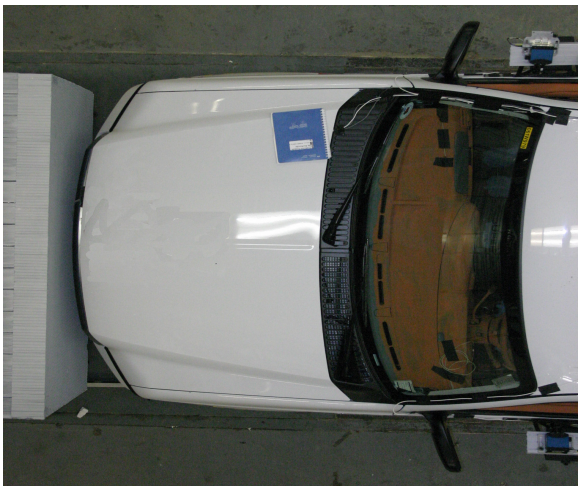

Figure 1A. Test setup for heavy-duty pick-up-to-barrier test: Top View.

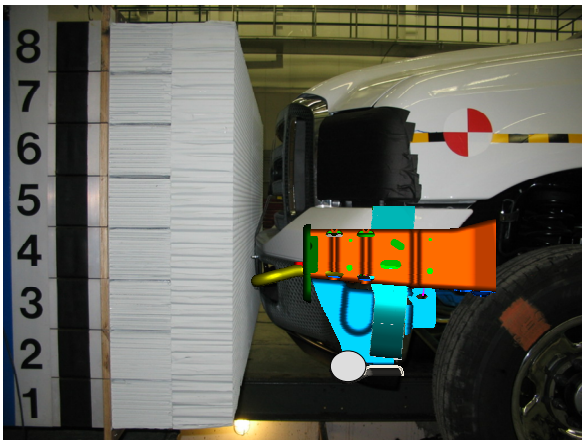

Figure 1B. Driver's side view of heavy-duty pick-up with SEAS showing key front structure and barrier.

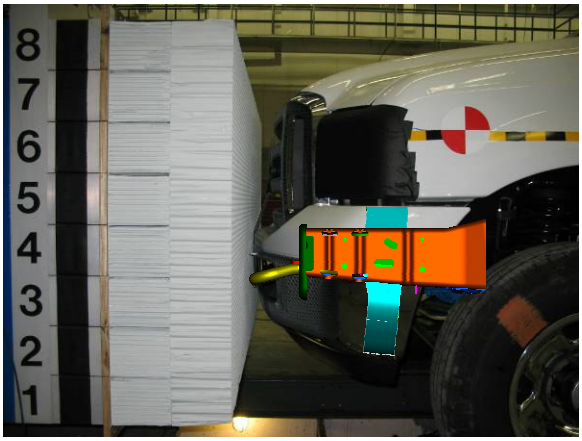

Figure 1C. Driver's side view of heavy-duty pick-up w/o SEAS showing key front structure and barrier.

The lower edge of the lowest row of load cells was 330 mm above the ground for the test. The impacting heavy-duty pick-ups with and without SEAS were aligned so that the vehicle centerline was aligned with the horizontal center of the barrier face (see Figure 1A). Figures 1B and 1C show the vertical height of front structure components and the lower radiator support structure. The primary energy absorbing structure (PEAS) is considered the front rails. The BlockerBeam® with attachment brackets as the secondary energy absorbing structure (SEAS) are also seen in the figures. The SEAS is directly attached to the front rails via these brackets as seen in Figure 1B.

Figure 2 shows a simplified CAD representation of the passenger side front rail and secondary energy absorbing structure along with the associated attachment bracket. The driver's side is similar. The SEAS and associated attachment bracket (Figure 2) were removed in the second test.

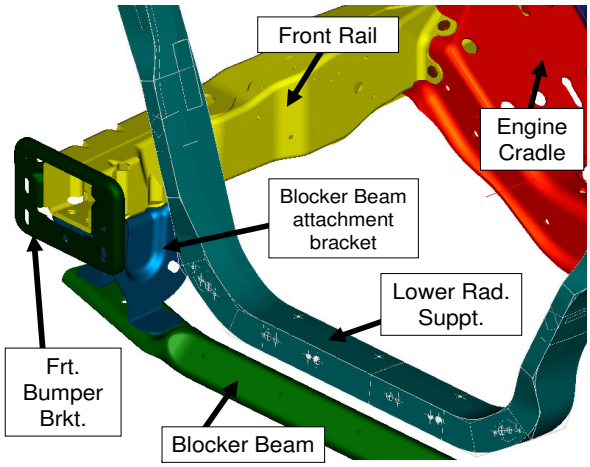

Figure 2. Front structure components in the heavy-duty pick-up.

Two full frontal NCAP tests against the LCW with deformable face at 57 kph were conducted with heavy-duty pick-ups. All vehicle parameters and test conditions (make, model, year model, body style, mass, impact speed, impact point etc.) were identical. The only difference in the two tests was the presence ("with SEAS") or absence ("without SEAS") of the secondary energy absorbing structures.

4. VEHICLE-TO-BARRIER: TEST RESULTS AND DISCUSSION

An objective of the current research is to evaluate the ability of the LCW with deformable face to detect the presence of SEAS such as the "BlockerBeam®" and to evaluate new or existing compatibility metrics. Figures 3 and 4 show the load-time history of each cell obtained from 57 kph impacts of heavy-duty pick-ups respectively. On the same figures it is also plotted the part 581 zone and locations of the PEAS and SEAS. Bigger percentage of the rail cross section (PEAS) falls in row 5 and some percentage in row 6.

The calculated AHOF values from both tests, with and without SEAS, are indicated on these figures. These values of the AHOF do not clearly discriminate the presence of SEAS. Figures 5 and 6 show the post impact deformation of the heavy-duty pick-ups with and without SEAS along with their corresponding barrier deformable faces respectively.

The major energy absorbing structure in smaller passenger cars falls mostly in rows 3 and 4 and therefore development of compatibility metrics should focus within these rows. Higher forces within rows 5 and 6 are generally evident as seen in Figures 3 and 4. Load cells near the PEAS record higher

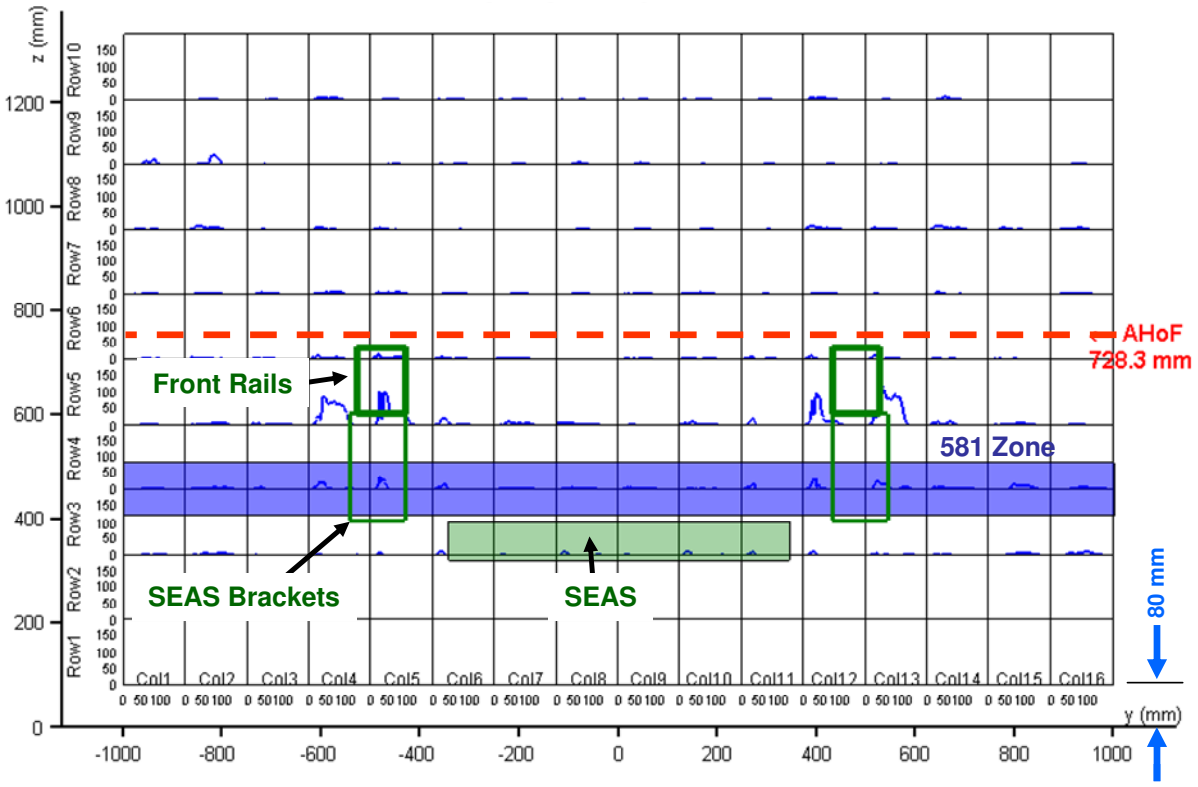

Figure 3. LCW force-time histories for heavy-duty pick-up with SEAS.

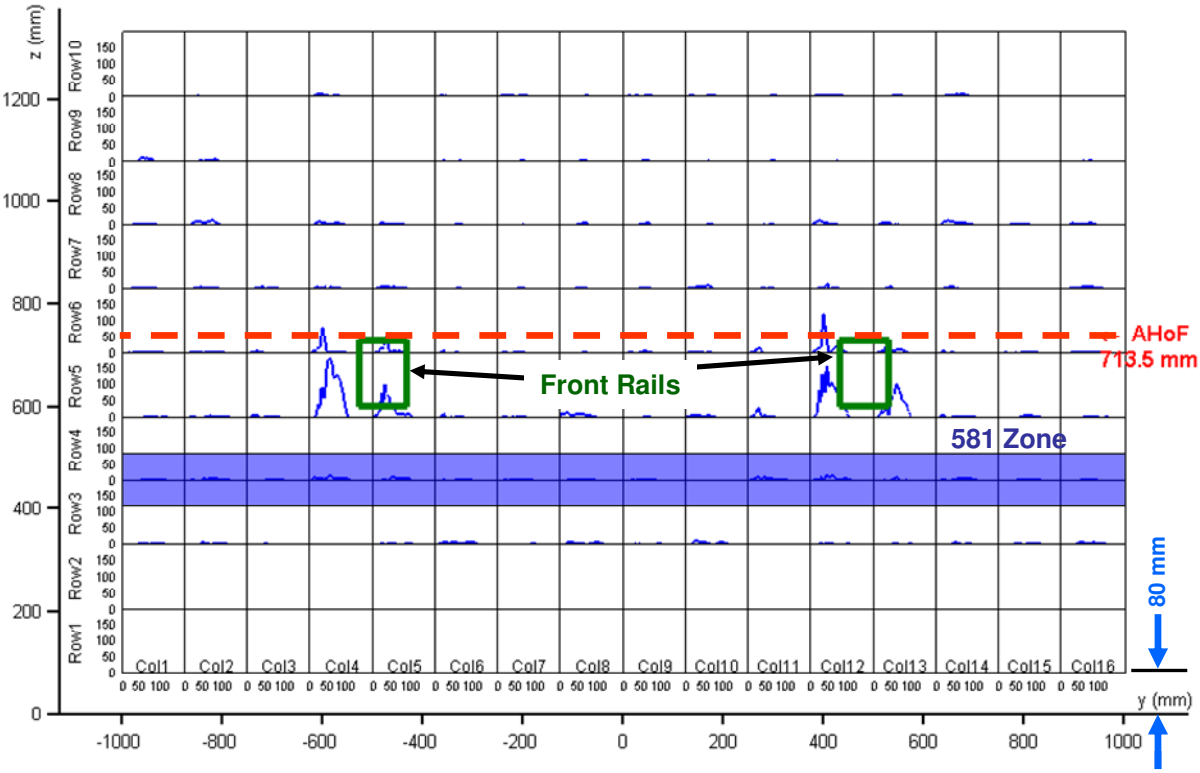

Figure 4. LCW force-time histories for heavy-duty pick-up without SEAS.

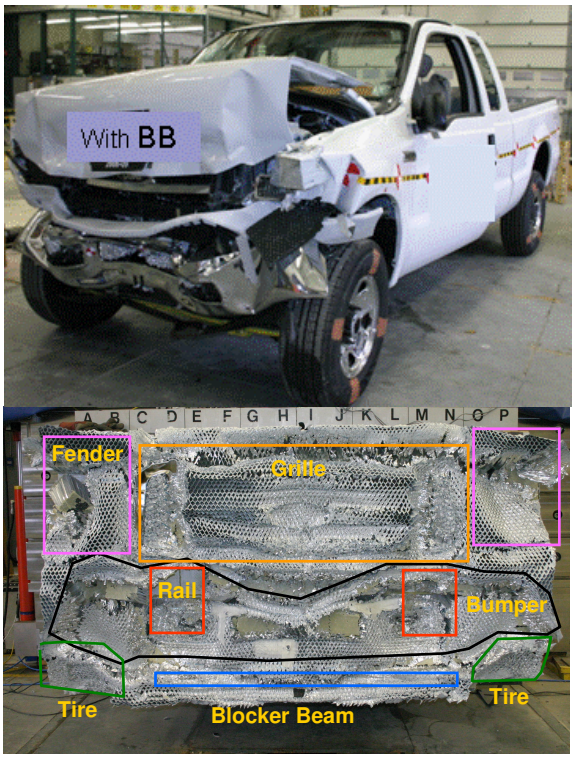

Figure 5. Post-impact pictures of the heavy-duty pick-up with SEAS and the corresponding barrier.

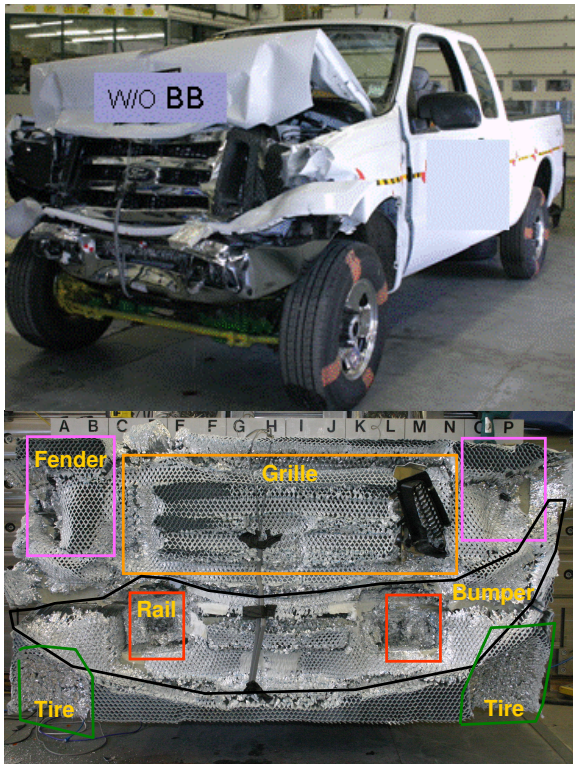

Figure 6. Post-impact pictures of the heavy-duty pick-up without SEAS and the corresponding barrier.

levels of forces than the surrounding cells. Additionally, the forces in PEAS associated cells for the heavy-duty pick-up with SEAS are lower than similar cells of the LCW when impacted by the heavy-duty pick-up without SEAS.

This is true because ideally the total LCW force should be the same due to impacts with the heavy-duty pick-ups with or without SEAS. However, LCW force profile seems to be slightly different indicating different collapse mechanisms of structure (see Figure 7). In cases where SEAS are present, wall cells around those structures will record more load as compared to cases where impact occurred without SEAS.

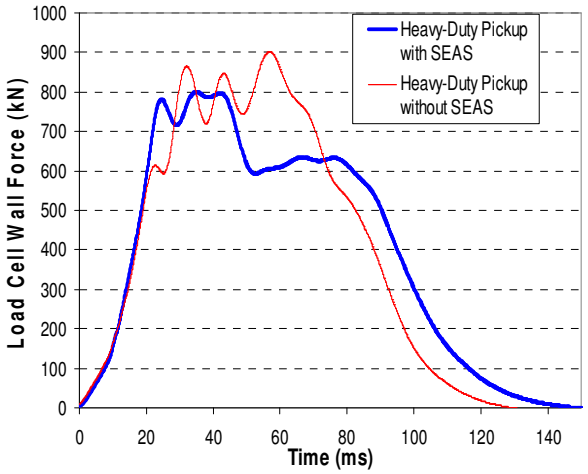

Figure 7. Time-history plots for the total barrier force of heavy-duty pick-ups with and without SEAS

Examination of the deformed vehicle and barriers faces (Figures 3-6) shows that the SEAS applied more load on rows 3 and 4 and resulted in less penetration into the deformable face with more load distribution. This is also evident from the observation of the deformed honeycomb faces in the tire, grille and bumper zones.

Figure 8 below gives the distribution of forces in rows 3 and 4 with respect to time for the heavy-duty pick-up with SEAS impact. For each row, all cells forces in that row are added with respect to time to form a row total force-time history in which the row's peak magnitude can be identified at a certain time. This differs from adding the peak force in each cell in a row, irrespective of the occurrence times, to find the row peak force magnitude. Figure 9 shows similar force-time history plots in rows 3 and 4 for the heavy-duty pick-up without SEAS impact.

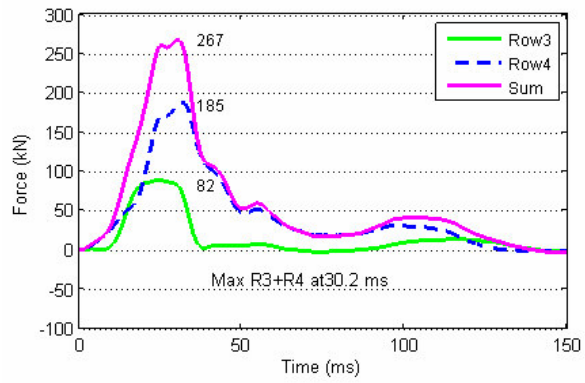

Figure 8. Force-time histories for rows 3 and 4 for the heavy-duty pick-up with SEAS.

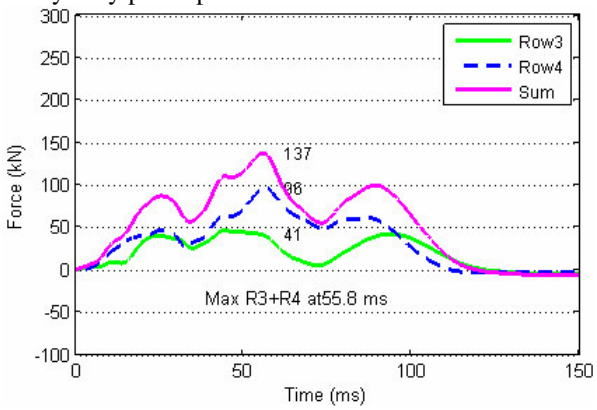

Figure 9. Force-time histories for rows 3 and 4 for the heavy-duty pick-up without SEAS.

A comparison between Figures 8 and 9 shows that rows 3 and 4 carry a significantly higher proportion of the load when the SEAS structure is present. It is also significant to note that the maximum force level of rows 3 and 4 combined occurs much later (at 55.8 ms as compared to 30.2 ms) without SEAS than with SEAS, respectively. This suggests that for developing a compatibility metric associated with peak row force magnitudes, it is suggested to restrict the window to one where the force peaks due to early interaction of the energy absorbing structures rather than due to engine engagement, which occurs later in the event. Therefore, a window of 0 to 40ms is recommended by this study as suggested by Edwards [10].

Figures 8 and 9 show that when the heavy-duty pick-up with SEAS impacts the LCW the SEAS structure transferred more of the dynamic force to lower portions (rows 3 and 4) of the LCW than when no SEAS. These figures also show that the difference in total load supported by rows 3 and 4 has a maximum magnitude of 130 KN. This is believed to be the force provided by the SEAS structure.

Figures 10 and 11 graphically show the dispersion of load horizontally across rows 3 and 4 for both pick-ups with and without SEAS respectively. The load dispersion in these rows is plotted at 30.2 ms and 55.8 ms for the case with and without SEAS respectively. These times correspond to the time the sum of the total forces in rows 3 and 4 is a maximum. The outer two load cells represented by columns 1, 2, 15, and 16 are omitted since very little load was recorded there. Figures 10 and 11 indicate the mean load levels in rows 3 and 4 were higher by nearly a factor of 2 when the pick-up impacting the LCW had SEAS than when it did not.

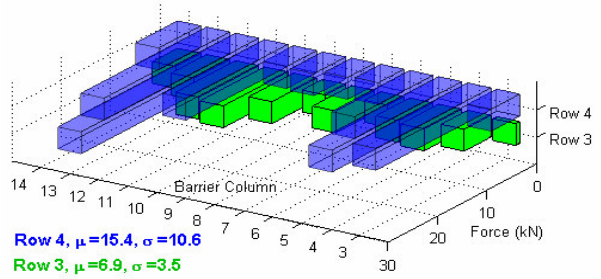

Figure 10. Horizontal load dispersion for the heavy-duty pick-up with SEAS at 30.2 ms.

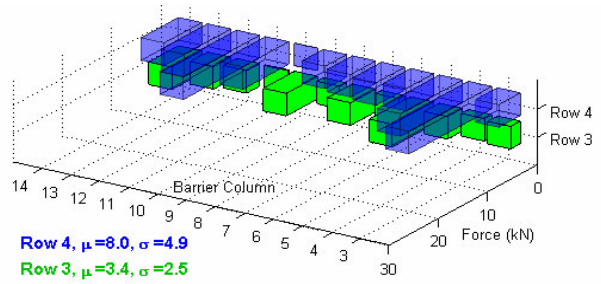

Figure 11. Horizontal load dispersion for the heavy-duty pick-up without SEAS at 55.8 ms.

Another approach for examining the horizontal force variation (similar to that seen in Figures 10 and 11) would be to find the peak force recorded in each load cell within a particular row independent of when it occurred. The results are shown in Figures 12 and 13 for rows 3 and 4 for the pick-ups with and without SEAS, respectively. Similarly, as with Figures 10 and 11, the average load levels seen in rows 3 and 4 are about twice as large when SEAS are present as when it is not.

In summary, the total maximum force appearing in a certain row, e.g. Row_i, can be characterized using two different methods. The force is denoted as the "Peak Load for Row_i" if the force time-histories from

all load cells within Row_i are combined to form a Row_i total force-time history, who's maximum value for a given time period is taken. If instead, the peak loads in each load cell within Row_i are first found irrespective of the precise time they occur and then summed, this force is denoted as "Sum of Peak Cell Loads for Row_i". In each method described, the values denoted by either "Peak Load for Row_i" or "Sum of Peak Cell Loads for Row_i" can be determined within a 40 ms time window. This leads to four different measures for a Row_i force.

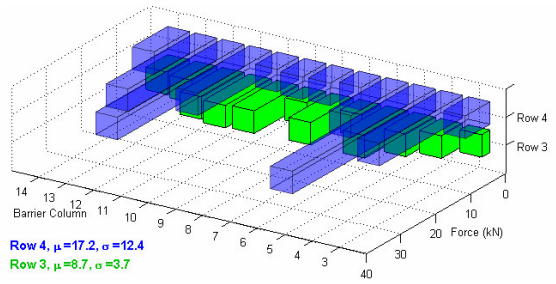

Figure 12. Peak load cell forces for the heavy-duty pick-up with SEAS (independent of time).

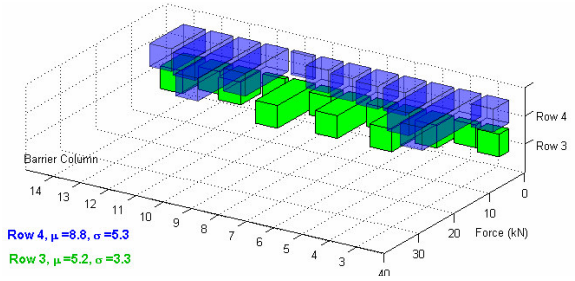

Figure 13. Peak load cell forces for the heavy-duty pick-up without SEAS (independent of time).

Figure 14 indicates that, for the heavy-duty pick-up with SEAS, the loads seen in rows 3-6 gradually increases and then decreases in approximately a 100-200-450-100 KN pattern. For the heavy-duty pick-up without SEAS, as seen in Figure 15, the loads in rows 3-6 build up gradually and in approximately a 50-50-400-300 KN pattern.

A shifting of load from rows 3 and 4 occurs when SEAS are absent since the total barrier load in both cases must remain the same (the impacting vehicle mass and velocity are the same). A noticeable increase occurs in row 5 due to the pick-up's frame or PEAS impact at this location. Additionally, there is more variability across the four measurement methods for row 5 when SEAS are not present (quantified in Figure 15). It should be noted that this load increase pattern is the same regardless of the method of calculation (Sum of Peak Loads vs. Peak Row), the only difference being the higher variability when SEAS is not present.

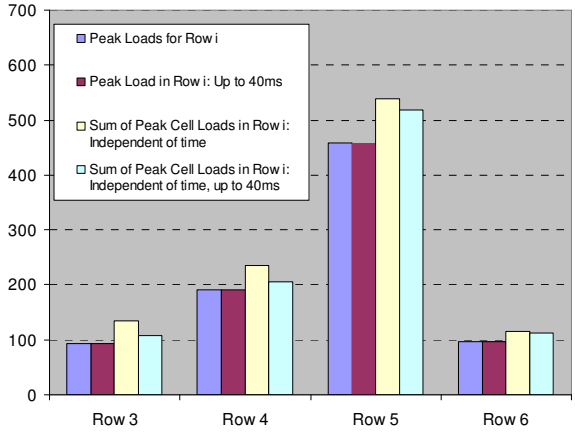

Figure 14. Peak loads in rows 3-6 for the heavy-duty pick-up with SEAS.

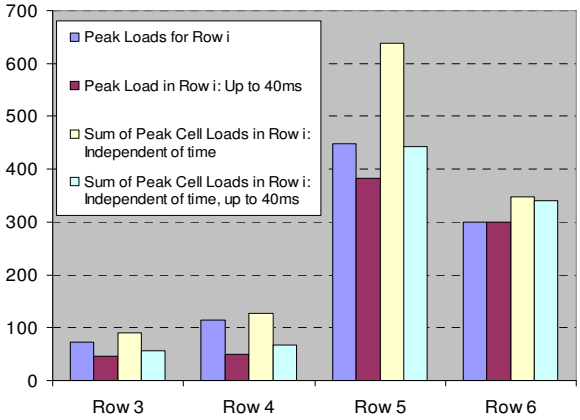

Figure 15. Peak loads for rows 3-6 for the heavy-duty pick-up without SEAS.

Edwards [10] has proposed row load based metrics VNT (Vertical Negative Deviation) and VSI (Vehicle Structure Interaction) as compatibility metrics. The aim of the vertical component is to ensure that there is sufficient vehicle structure in alignment with the common interaction area, rows 3 and 4. It sets a target row load of 100 KN minimum and calculates the load below the target row. The VNT is essentially characterized by the sum of peak force method and the VSI are generally characterized by the same sum of peak values up to 40 ms.

In the current research the authors attempt to evaluate the VNT and VSI metrics using the LCW discussed results (Figures 3-15) and results obtained from heavy-duty pick-ups with and without SEAS in full frontal impacts against a small passenger car.

Since the sequence of structural component collapse is important and depends on time, the current authors suggest and prefer to use the time-dependent "Peak Load for Row_i" instead of non-time dependent "Sum of Peak cell Loads for Row_i" to calculate the VNT and VSI. It is preferred that if lower bounds for force level are intended for row load targets, conservative or minimum values should be used. The sum of peak values will always be greater than or equal to the peak row loads for any given row (e.g. the peak row load is a lower bound for the sum of peak cell loads for any row). Since in vehicle-to-vehicle impact compatibility focuses on front-end structural interactions and not those from the engine, a window of 40ms is recommended here.

Figures 8, 9, 14, and 15 clearly show that the peak row loads using a 40ms window limit can distinguish the presence of SEAS. The force levels seen in rows 3 through 6 indicate that the SEAS shifted a good percentage of the total barrier load into rows 3 and 4. A target load of 100KN on rows 3 and 4 has a potential to discriminate presence of SEAS. Table 4 below contains the calculated compatibility measures.

Table 4: Summary of Vertical and Horizontal Negative Deviation Measures

			Heavy Duty Pickup with SEAS	Heavy Duty Pickup without SEAS
Verticle Metrics		AHOF	728.3	713.5
		AHOF400	694.6	743.6
	Approx. VNT	Σ peak cell loads in Row 3, all time	134.5	90.5 **< 100**
		Σ peak cell loads in Row 4, all time	235.5	127.5
	Approx. VSI	Σ peak cell loads in Row 3, t < 40 ms	108.0	56.2 **< 100**
		Σ peak cell loads in Row 4, t < 40 ms	205.5	66.5 **< 100**

5. VEHICLE-TO-VEHICLE TEST SETUP AND PROCEDURES

The test configuration of full frontal collinear vehicle-to-vehicle impact is shown in Figure 16. Figure 17 shows a close-up view of the geometrical alignments and differences between structural front-end components of the impacted vehicles. Two tests were conducted with the target vehicles chosen to be the same (small size passenger cars) while the bullet vehicles were selected to be heavy-duty pick-ups with and without SEAS. The bullet pick-ups were identical to those used in LCW tests and had identical characteristics and specifications. All vehicles were fully instrumented. Dimensional analyses points and sections were specified on all vehicles for pre- and post-crash deformation analyses. The target vehicle was initially at rest in both tests. The bullet vehicle's velocity was selected based on the relative masses involved, i.e., the bullet vehicle impact velocity was mass adjusted to 82 kph in order to induce a 56 kph barrier-equivalent velocity (BEV) in the target vehicle. The 56 kph BEV was selected to model the test conditions of NCAP.

In all the Pick-up-to-Car tests, both the bullet and target vehicles used a Hybrid III 50th percentile, male dummy in the driver mid position and a Hybrid III 5th percentile, female dummy in the passenger full forward position. All the dummies were belted and the airbags were active. A summary of test conditions for the two vehicle-to-vehicle tests is given in Table 5. Figure 16 shows top and side views of the test setup prior to impact.

Table 5: Vehicle-to-Vehicle Test Conditions

	Test 1		Test 2	
	Heavy-Duty Pickup with SEAS	Small Passenger Car	Heavy-Duty Pickup **without** SEAS	Small Passenger Car
Model Year	2007	2005	2007	2005
Vehicle Weight	3191 kg	1531 kg	3186 kg	1538 kg
Vehicle Ride Height (mm, RH / LH)	1010 / 1000	647 / 641	1002 / 994	658 / 654
Impact Velocity	82.55 kph	0.0	83.05 kph	0.0
Velocity Change	26.71 kph	55.84 kph	27.04 kph	56.02 kph

Figure 16. Top and side views of the vehicle-to-vehicle test set-up.

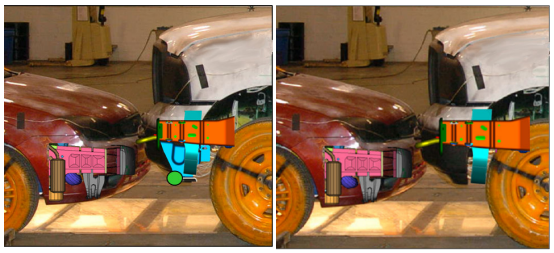

Figure 17. Views of PEAS and SEAS geometrical differences between target and bullet vehicles.

6. VEHICLE-TO-VEHICLE TEST RESULTS AND DISCUSSION

Evaluation of proposed compatibility metrics (VNT and VSI) obtained from LCW tests and their correlation with target vehicle's occupant responses and intrusions obtained from vehicle-to-vehicle impact was the primary objective of this study. Unfortunately, most of the driver dummy's and some of the passenger dummy's channel recordings were lost in the test of the heavy-duty pick-up with SEAS against a passenger car due to a high voltage anomaly. Therefore, only vehicle decelerations, displacements, and intrusions will be used for the correlation and conclusions. The authors' plan is to repeat the test and successfully collect all dummy responses for use in correlation of the compatibility metrics with occupant responses. The results will be reported in future publications.

6.1 Vehicle Deceleration Pulse Comparisons

Figures 18 and 19 show the comparison of the deceleration pulses of the target and bullet vehicles resulting from the 82 kph full frontal impacts by heavy-duty pick-ups with and without SEAS respectively.

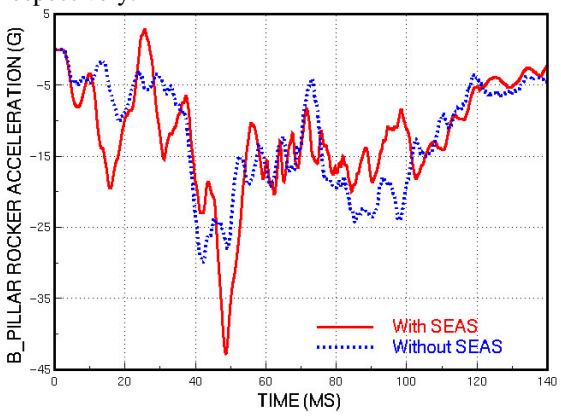

Figure 18. A comparison of target vehicle pulses.

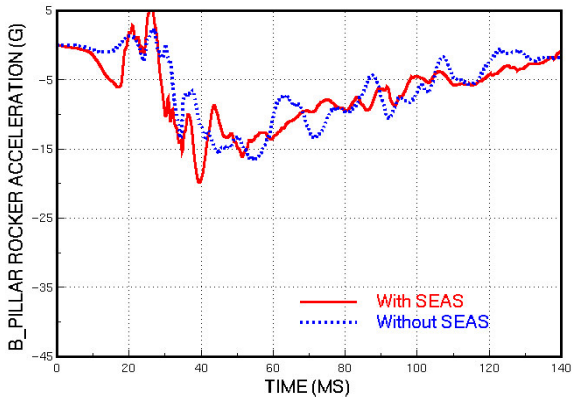

Figure 19. A comparison of bullet vehicle pulses.

The effect of the presence of SEAS is quite obvious from Figures 18 and 19. The SEAS on the striking heavy-duty pick-up engages the front end PEAS of the passenger car and transmit a larger force to the target vehicle early in the impact event, less than 20 ms, as seen in these figures. SEAS cause the 20 G deceleration at approximately 20 ms experienced by the target vehicle.

From Newton's law, by considering the mass times the deceleration, approximately 304 KN of force is acting on the vehicles at this particular time. Such force level was observed in the interaction zone (rows 3 and 4) in the LCW test impacted by the heavy-duty pick-up with SEAS (see Table 4). The target vehicle experienced a much lower deceleration level when impacted by the heavy-duty pick-up without SEAS, Figure 18. This means that within 20-25 ms of initial impact, the pick-up missed engagement with the passenger car PEAS and contacted the passenger car's engine at approximately 30 ms. This is evident from the sudden jump of the crash pulses in both the target and bullet vehicles as seen in Figures 18 and 19, respectively.

6.2. Correlation Between LCW and Vehicle-to-Vehicle Results for Proposed Metrics Evaluation

In the LCW deformable barrier tests it was shown in Table 4 that the heavy-duty pick-up with SEAS delivered forces in rows 3 and 4 around 100 KN and 200KN respectively. The force in the interaction zone between two impacted vehicles characterized by rows 3 and 4 can total to about 300 KN. This force is acting on the PEAS of the target vehicle and reacted on the SEAS of the bullet vehicle during approximately the first 40 ms of impact.

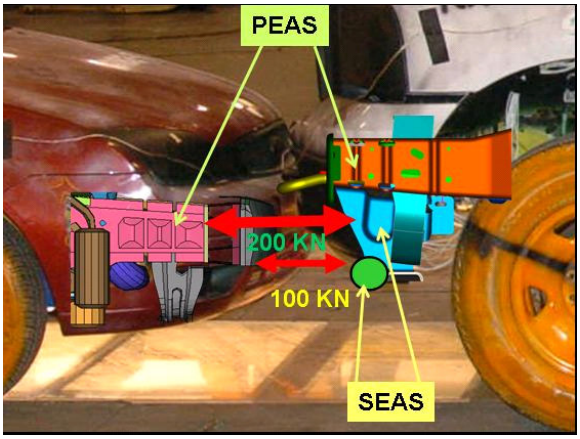

Figure 20. Forces in the interaction zone between the target and bullet vehicles.

This force level acting on the target vehicle is both sufficient to crush the front part of its PEAS and to deform the SEAS of the bullet vehicle, represented by the BlockerBeam® and its attachment brackets. It is always recommended to have both vehicles involved in the crash absorb some energy. Figure 20 shows a graphical representation of the force acting on both vehicles.

6.3. Comparison of Overall Deformation of Target and Bullet Vehicles

Figures 21 and 22 show the overall deformations of the bullet and target vehicles with and without SEAS in the bullet vehicle. Examining the bullet vehicles it is shown that the vehicle with SEAS experienced more deformation in the bumper and grille areas compared to that without SEAS. This is due to more structural interaction between the front-ends of the impacting vehicles in the case of the impact with SEAS compare to that without SEAS.

The target vehicle impacted by the bullet with SEAS has less overall deformation compared to that impacted by bullet without SEAS (Figures 21 and 22). This is very clear in the deformation zone around the A-pillar/roof rail and B-pillar roof rail joints. This is due to a greater override of the bullet vehicle onto the target when the SEAS is removed.

Figure 21. Post impact pictures of the bullet and target vehicles with SEAS on the bullet vehicle.

Figure 22. Post impact pictures of the bullet and target vehicles with no SEAS on the bullet vehicle.

Figure 23 is a CAD representation of the un-deformed shape of the front-end and engine of the target vehicle. Figures 24 and 25 show the specific collapse modes of the PEAS of the target passenger vehicle impacted by the bullet vehicle with and without SEAS. Axial collapse is first observed in the target vehicle's fore-rail followed by a bending collapse near the engine mount due to the presence of SEAS and better structural interactions (see Figure 24). In the second test with the SEAS removed, the bullet vehicle's PEAS missed the front portion of the target vehicle's rail causing more override that resulted in excessive rotation and bending of aft rail of the target vehicle as shown in Figure 25.

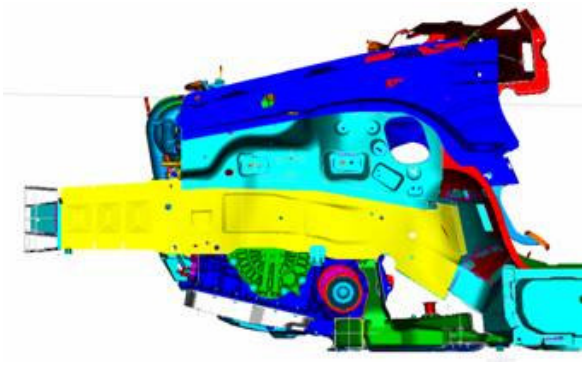

Figure 23. The undeformed shape of the front-end and engine of the target vehicle.

Comparing Figures 24 and 25, it is evident that the presence of SEAS resulted in less rotation of the spring box and engine. This is due to less override and more structural interaction that led to less structural intrusions in general.

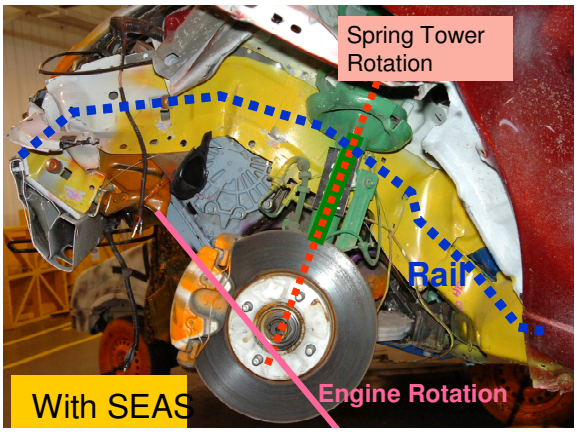

Figure 24. The post crash deformation of the front-end structure and engine rotation in the target vehicle impacted by bullet vehicle with SEAS

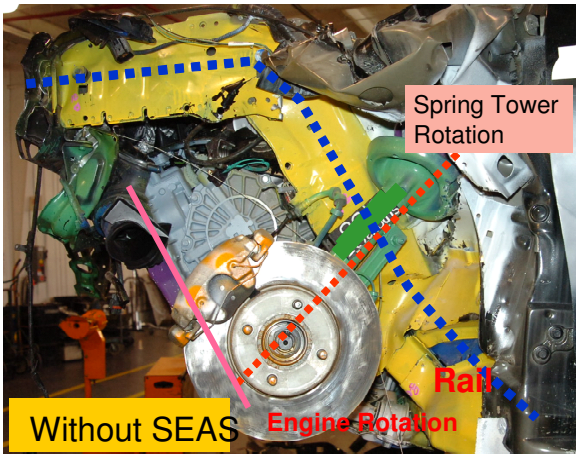

Figure 25. The post crash deformation of the front-end structure and engine rotation in the target vehicle impacted by bullet vehicle without SEAS.

6.4. Comparison of Vehicles Displacement During Impact

The crash pulses of both target and bullet vehicles shown in Figures 18 and 19 were double integrated to obtain their corresponding displacements. Figure 26 shows displacement of the target and bullet vehicles for the case of the heavy-duty pick-up with SEAS impacting a small size passenger car. Similarly, Figure 27 shows the displacements resulting from the heavy-duty pick-up without SEAS impacting a similar small size passenger car.

In Figures 26 and 27, the difference between the two curves represents relative displacement between points on the B-pillar/rocker on the bullet and target vehicles involved in the crash. This difference includes deformation and override. The maximum relative displacement happened at the rebound time when the two vehicles began to separate.

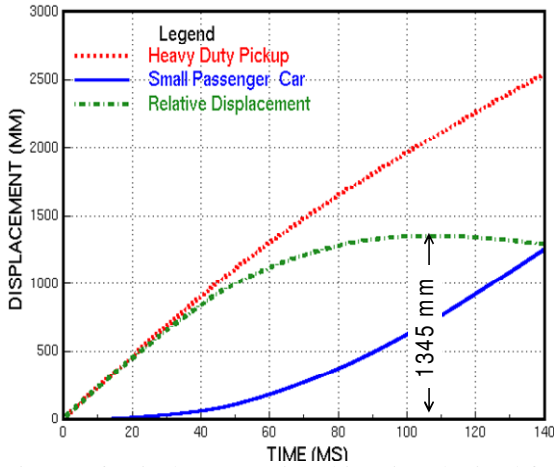

Figure 26. Displacement time-histories obtained from bullet vehicle with SEAS-to-target vehicle impact.

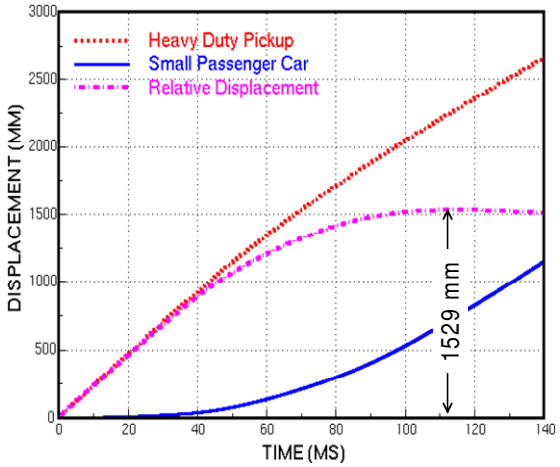

Figure 27. Displacement time-histories obtained from bullet vehicle without SEAS-to-target vehicle impact.

Comparing Figures 26 and 27 it is evident that the maximum relative displacement in the absence of SEAS is 184 mm more than that with SEAS (1529 mm vs. 1345 mm). This indicates that there is more override over the target vehicle and more intrusion resulted in the case of no SEAS compared to that with SEAS.

6.5. Dimensional Analyses

Pre-and post-crash dimensional analyses on target vehicles impacted by bullet vehicles with and without SEAS were carried out to obtain intrusion profiles shown in Figures 28 and 29 respectively. Intrusion profiles represented by sections from the cowl top to the floor panel at the driver centerline, vehicle centerline and passenger centerline are shown in Figures 30-32.

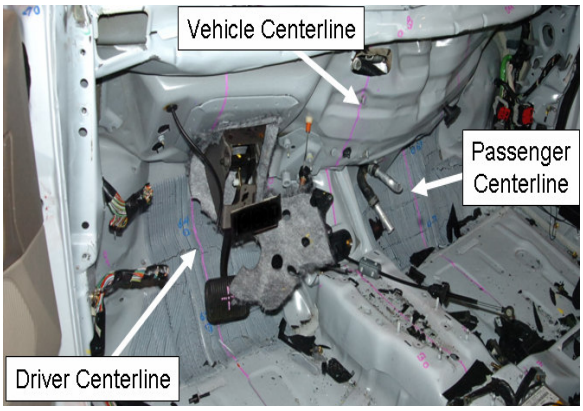

Figure 28. Post-crash sections on target vehicle impacted by the bullet vehicle with SEAS.

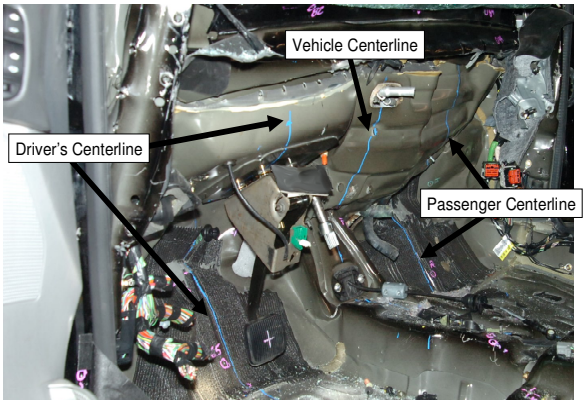

Figure 29. Post-crash sections on target vehicle impacted by the bullet vehicle without SEAS.

In Figure 30 it is evident that having the SEAS on the bullet vehicle has significantly reduced cabin intrusions at the driver centerline, specifically at the instrument panel area due to improved structural interactions and reduced override. Higher engine rotation in the target vehicle when impacted by the bullet vehicle without SEAS caused larger upper dash intrusions. Figure 31 shows a small difference between the dash intrusion profiles on the target vehicle caused by the bullet vehicles with and without SEAS at the vehicle centerline.

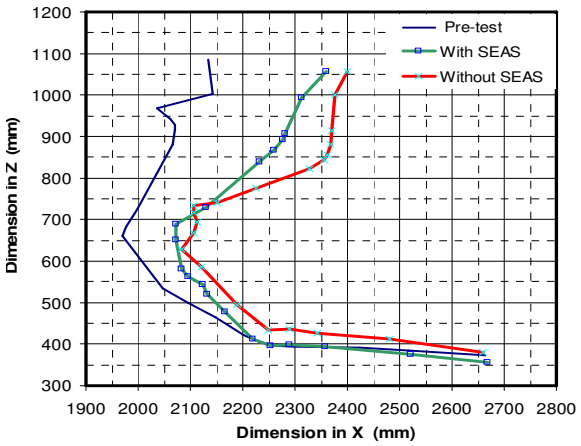

Figure 30. Dash intrusion for the target vehicle at the driver's centerline.

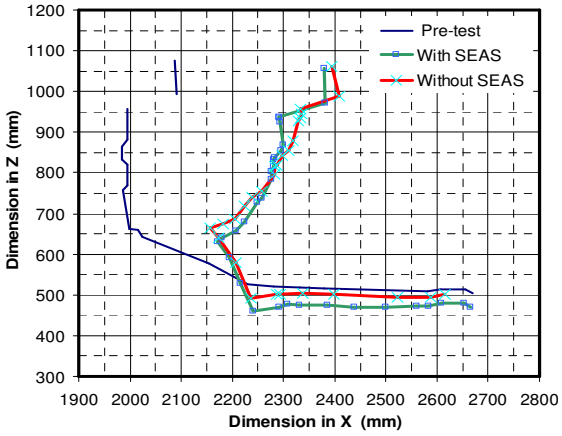

Figure 31. Dash intrusion for the target vehicle at the vehicle centerline.

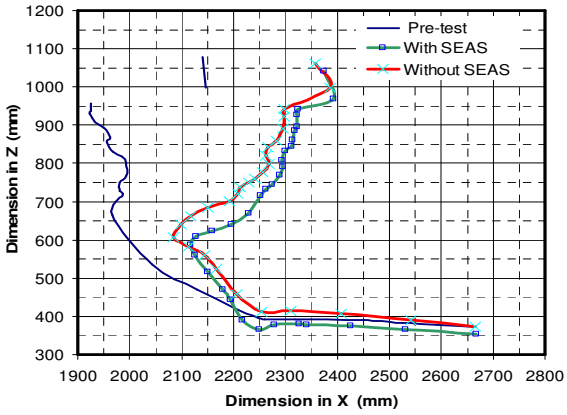

Figure 32. Dash intrusion for the target vehicle at the passenger centerline.

For the passenger centerline intrusions, Figure 32 shows mixed results. Intrusions are improved in the

lower part of the cabin at the foot pedal and foot rest areas with the presence of SEAS. Intrusions at the upper part get worse near instrument panel area. Very careful examination of the post-crashed target vehicles was conducted to better understand this observation. The engine is transversely mounted and is pivoted at a point approximately one-third of its transverse dimension towards the driver side and two-third towards the passenger side. In the case of the pick-up with SEAS impact, higher forces were transmitted to the engine in the interaction zone compared to that without SEAS. This caused more rotation of the intruded engine towards the passenger side.

Post-crash deformation of significant points in the target vehicle, such as points on fore rail, mid rail, bumper mounting, and spring tower, impacted by bullet vehicles with and without SEAS are presented in Figure 33. Having the SEAS provided significant improvement in reducing the intrusions at these points.

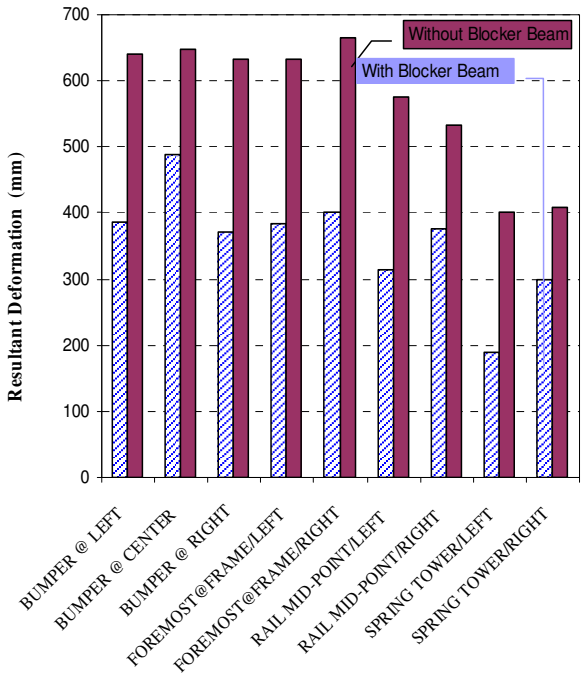

Figure 33. Resultant deformation of points on the target vehicle's primary structure.

Figures 34 and 35 present the dimensional analyses of the pre- and post-crash of the target vehicle's passenger compartment resulting from impact with bullet vehicles with and without SEAS. In Figure 34, A represents a point at the A-pillar/roof joint, B represents a point at the B-pillar/roof joint, C represents a point at B-pillar/beltline, D represents a point at the B-pillar/rocker joint, E represents a point at the A-pillar/rocker joint, and F represents a point at the A-pillar/beltline. It is indicted from this figure that the presence of SEAS provided significant improvement in reducing the override which led to less overall deformation and intrusions in the passenger compartment of the target vehicle.

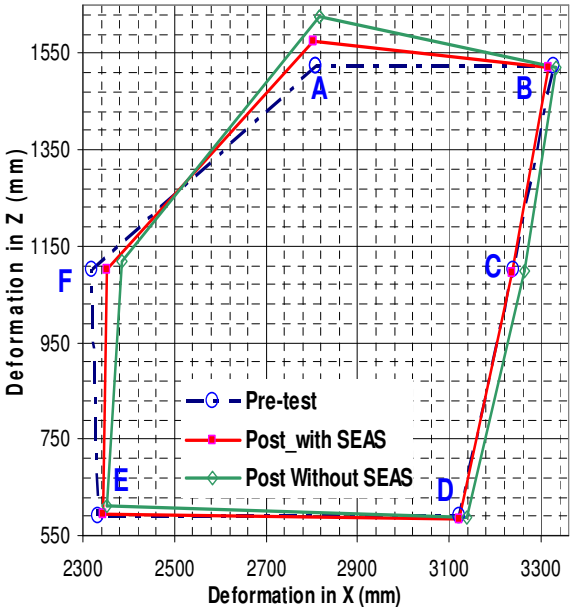

Figure 34. Passenger compartment deformation of the target vehicle impacted by bullet vehicle with and without SEAS.

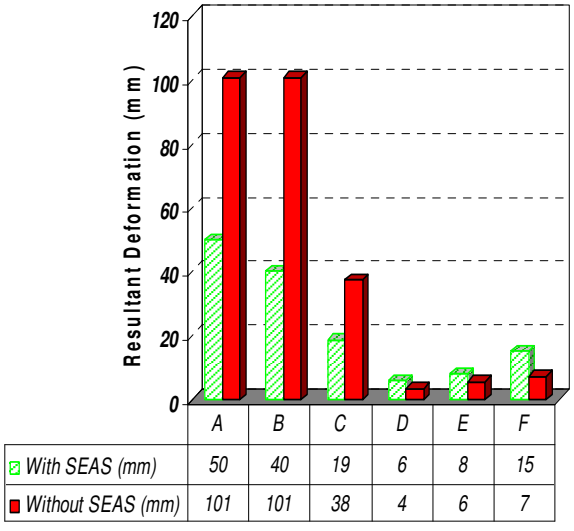

	A	B	C	D	E	F
With SEAS (mm)	50	40	19	6	8	15
Without SEAS (mm)	101	101	38	4	6	7

Figure 35. Resultant deformation of points at joints on the target vehicle's cabin impacted by bullet vehicles with and without SEAS.

7. CONCLUSIONS

- Real-world accident data analyses had been conducted to evaluate the effectiveness of Ford's BlockerBeam® (a Secondary Energy Absorbing Structures, SEAS, one of the recommendations of TWG) in vehicle-to-vehicle frontal and side crashes. A comparison of the collision performance between LTVs with and without Ford's BlockerBeam® showed a significant reduction in fatality rates for vehicles with the added BlockerBeam® in frontal impact. This data by itself is not sufficient to identify a single factor as the cause for this reduction. Results also showed significant reduction in the fatality rate in the struck vehicle when the striking LTVs has Ford's BlockerBeam® in near side impact.
- Vehicle-to-barrier and vehicle-to-vehicle crash tests were conducted to develop assessment procedures and metrics that can be used to predict compatibility performance.
- Heavy-duty pick-ups with and without SEAS were tested in the NCAP configuration against high resolution LCW with a deformable face to detect the presence of SEAS (BlockerBeam®) and to evaluate potential compatibility metrics.
- LCW results showed that the heavy-duty pick-up with SEAS helped in transferring dynamic force to lower portions (rows 3 and 4) of the LCW. Results obtained from pick-up impacts with and without SEAS identified a difference in total load supported by rows 3 and 4 of 130 KN. This force may be attributed to the SEAS structure.
- In calculating metrics such as VNT, VSI or other potential force-based metrics, it is suggested to use the time-dependent peak load instead of non-time dependent sum of the peak cell loads.
- The peak row loads using a 40ms time limit can distinguish the presence of SEAS. A target load of 100KN on rows 3 and 4 has a potential to discriminate presence of SEAS.
- 82 kph full frontal collinear impacts of bullet vehicles (heavy-duty pick-ups with and without SEAS) against a stationary target vehicle (small size passenger car) were also conducted. Barrier test results and associated metrics were correlated to results obtained from vehicle-to-vehicle tests for assessment of compatibility measures and test procedures.
- During the first 40 ms in vehicle-to-vehicle impact when the bullet vehicle has SEAS, approximately 304KN of force acts on the vehicles in the interaction zone. This force level is correlated to that observed in the interaction zone (rows 3 and 4) in the LCW test impacted by the heavy-duty pick-up with SEAS.
- The presence of the SEAS on the bullet vehicle provided good interaction with the PEAS of the target vehicle. This led to reduction in override of the target vehicle that resulted in significant reduction of the overall deformations and intrusions in the target vehicle's passenger compartment.
- Finally, the LCW with deformable face investigated in this study has a potential to be used to assess vehicle compatibility.

8. ACKNOWLEDMENT

The authors would like to acknowledge Kay Sullivan and Scott Henry from the Automotive Safety Office at Ford for their contribution to the accident data analyses to evaluate the effectiveness of Ford's BlockerBeam®. The authors wish to thank Ms. Suzanne Tylko of Transport Canada and Mr. Alain Bussières of PMG for conducting the vehicle-to-barrier tests.

9. REFERENCES

[1] Barbat, S. 2005. "Status of Enhanced Front-To-Front Vehicle Compatibility Technical Working Group Research and Commitments", 19th ESV Conference, Washington, D.C., Paper No. 05-463.

[2] Auto Alliance, 2003. "Enhanced Vehicle-to-Vehicle Crash Compatibility: Commitment for Continued Progress by Leading Automakers".

[3] Barbat, S., Li, X., and Prasad, P. 2001. "Evaluation of Vehicle Compatibility in Various Frontal Impact Configurations." 17th ESV, Amsterdam. Netherlands. Paper No. 01-S7-O-09.

[4] Barbat, S., Li, X., and Prasad, P. 2001. "A Comparative Analysis of Vehicle-to-Vehicle and Vehicle-to-Rigid Fixed Barrier Frontal Impact." 17th ESV, Amsterdam, Netherlands. Paper No. 01-S7-O-01.

[5] Edwards, M., Davies, H., and Hobbs, A. 2003. "Development of Test Procedures and Performance Criterion to Improve Compatibility in Car Frontal Collisions", 18th ESV Conference, Nagoya, Japan, Paper No. 86.

[6] Diggs, K., Eigen, A., and Harrison, J., 1999. "Application of Load Cell Barrier Data to Assess Vehicle Crash Performance and Compatibility", SAE, Warrendale, PA, 1999-01-0770.

[7] Summers, S., Prasad, A., and Hollowell, W.T. 2001. “NHTSA’s Compatibility Research Program Update”, SAE, Warrendale, PA, 2001-01-1167.

[8] Summers, S., Hollowell, W.T. and Prasad, A. 2002. “Design Considerations for a Compatibility Test Procedure”, SAE, Warrendale, PA, 2002-01-1022.

[9] Verma, M. 2007. “Enhanced Vehicle Collision Compatibility – Progress Report of US Technical Workgroup for Front-to-Front Compatibility”, 20th ESV Conference, Lyon, France. Paper No. 07-0291.

[10] Edwards, M., Cuerden, R., and Davies, H. 2007. "Current Status of the Full Width Deformable Barrier Test", 20th ESV Conference, Lyon, France. Paper No. 07-0088